Nano-Kelvin Thermometry and Temperature Control: Beyond the Thermal Noise Limit

Wenle Weng,[1,2,*] James D. Anstie,[2,1] Thomas M. Stace,[3] Geoff Campbell,[4] Fred N. Baynes,[1] and Andre N. Luiten[2,1]
[1]School of Physics, University of Western Australia, Western Australia 6009, Australia
[2]Institute for Photonics and Advanced Sensing and School of Chemistry and Physics, University of Adelaide, South Australia 5005, Australia
[3]School of Mathematics and Physics, University of Queensland, Brisbane, Queensland 4072, Australia
[4]Department of Quantum Science, Australian National University, Australian Capital Territory 0200, Australia
(Received 16 July 2013; revised manuscript received 13 February 2014; published 21 April 2014)

We demonstrate thermometry with a resolution of 80 nK/$\sqrt{\text{Hz}}$ using an isotropic crystalline whispering-gallery mode resonator based on a dichroic dual-mode technique. We simultaneously excite two modes that have a mode frequency ratio that is very close to two (±0.3 ppm). The wavelength and temperature dependence of the refractive index means that the frequency difference between these modes is an ultrasensitive proxy of the resonator temperature. This approach to temperature sensing automatically suppresses sensitivity to thermal expansion and vibrationally induced changes of the resonator. We also demonstrate active suppression of temperature fluctuations in the resonator by controlling the intensity of the driving laser. The residual temperature fluctuations are shown to be below the limits set by fundamental thermodynamic fluctuations of the resonator material.

DOI: 10.1103/PhysRevLett.112.160801 PACS numbers: 07.20.Dt, 42.60.Da, 42.62.Fi

The high-resolution measurement of energy has long fascinated humans with its culmination seen in ultra-high-sensitivity calorimeters [1,2] and bolometers [3]. These and related ideas have found a broad range of applications, including bolometric superconducting photon counters for quantum communication [4] and ultrasensitive radio astronomy [5,6]. The record for absolute thermometric sensitivity has been realized at cryogenic temperatures, achieving better than 100 pK/$\sqrt{\text{Hz}}$ [7].

In this Letter, we develop a new method to measure temperature based on excitation of two well-separated modes in a millimeter-scale whispering-gallery (WG) optical resonator. WG mode resonators have exceptionally high Q factors and can provide the potential of providing high-stability microwave and optical signals [8–12]. Recently, they have been applied to high-sensitivity label-free sensors for molecules and viruses [13,14] and for optical comb generation [15]. Nonetheless, an issue that afflicts all of these applications is the high temperature sensitivity of WG resonators [12,16], particularly when compared to conventional vacuum-spaced Fabry-Perot resonators [17–21]. In this Letter, we turn this problem to our advantage by using the WG resonator as an ultrasensitive thermometer.

To suppress unwanted temperature fluctuations in WG resonators, several groups have demonstrated *in situ* thermometry by measuring the frequency difference between two orthogonally polarized modes. The best of these techniques have demonstrated a resolution of ~100 nK/$\sqrt{\text{Hz}}$ [22], and subsequent temperature stabilization based on this sensing has resulted in improvement to the long-term frequency stability [23,24]. In contrast, we present a two-color approach to measure the resonator temperature with high resolution. In comparison to the birefringent dual-mode technique, our approach can be used in both anisotropic and isotropic resonators, which expands the range of material candidates. Isotropic materials have shown the highest Q factors to date [25], which offers a potentially higher temperature resolution. On the other hand, a combination of the dual-color and dual-polarization approaches in an anisotropic material (e.g., MgF_2) can further enhance the temperature sensitivity. Furthermore, our dual-color technique strongly rejects noise from thermal expansion fluctuations and vibrations, giving us the ability to measure the mode-averaged temperature with a resolution below that of the fundamental thermal temperature fluctuations [16,26,27].

The frequency of a WG mode depends on temperature through (a) the temperature dependence of the refractive index (thermooptic effect) as well as (b) the thermal expansion of the resonator. The first dependence leads to sensitivity to the temperature solely within the optical mode, whereas in the latter, the mode frequency depends on the temperature distribution throughout the entire resonator volume. For simplicity, we assume a steady-state temperature distribution, $T_P(r)$, when the resonator is excited by some input optical power, P, that is solely dependent on the radial coordinate, r. This approximation reflects the typical triple cylindrical symmetry exhibited by the (a) resonator geometry, (b) optical power distribution, and (c) thermal coupling to the external environment. When the power-induced temperature changes from ambient are small [i.e., $\Delta T_P(r) = T_P(r) - T_0(r) \ll T_0(r)$], we can express the frequency, f_m, of the mth mode as

$$\frac{f_m}{f_{m,0}} = 1 - \frac{2\alpha \int_0^R \Delta T_P(r) r dr}{R^2} - \frac{\beta(f_m)}{n(f_m)} \Delta T_P(R) - \gamma_m, \quad (1)$$

where $f_{m,0}$ is the frequency of the mth mode in the absence of excitation power, α is the linear thermal expansion coefficient, and $\beta(f_m)$ and $n(f_m)$ are the thermooptic coefficient and refractive index of the resonator material, respectively, R is the radius at the mode intensity maximum, and $\gamma_m = (2Q_0/(Q_0 + Q_c))(n_{\mathrm{Kerr}}/n(f_m))(\mathcal{F}/\pi)(P/A_m)$ characterizes the refractive index dependence on the optical intensity, which depends on the Kerr coefficient n_{Kerr}, and finesse $\mathcal{F}$ [28]. Q_0 and Q_c are the intrinsic Q factor and coupling Q factor, respectively. We define an effective mode area $A_m = (\int |E_m|^2 dA \int |E_{\mathrm{tot}}|^2 dA / \int |E_m|^2 |E_{\mathrm{tot}}|^2 dA)$, where E_m is the amplitude of the mth mode in the transverse plane and E_{tot} is the field amplitude of the resonant energy (which allows for more than one mode to be excited simultaneously).

The basis of our thermometer is to simultaneously lock two optical signals to two WG modes that have frequencies f_1 and f_2 with $f_2 \approx 2f_1$. These modes are chosen to be within the same transverse mode family (i.e., identical polar and radial field maxima numbers [29]) to maximize their spatial overlap.

For simplicity, the two optical signals are derived from a single laser with frequency f_L. The direct output of the laser is locked using the Pound-Drever-Hall (PDH) technique [30] to the lower frequency WG mode, i.e., $f_L = f_1$. We frequency double this laser signal and shift it into resonance with the second WG mode using an acousto-optic modulator (AOM) so that $2f_L + f_{\mathrm{AOM}} = f_2$. From Eq. (1), it follows that

$$f_{\mathrm{AOM}} \approx 2f_L \left(\frac{\beta(f_1)}{n(f_1)} - \frac{\beta(f_2)}{n(f_2)} \right) \Delta T_P(R) + C + \Gamma + N, \quad (2)$$

where $C = f_{2,0} - 2f_{1,0}$ is a constant frequency offset, $\Gamma = 2f_L(\gamma_1 - \gamma_2)$ is the relative nonlinear Kerr shift, and $N = \delta f_2 - 2\delta f_1$, which accounts for residual errors in the laser locking systems, i.e., $\delta f_1 = f_L - f_1$ and $\delta f_2 = 2f_L + f_{\mathrm{AOM}} - f_2$. Importantly, the high degree of spatial overlap between the two modes gives rise to nearly identical frequency dependence on thermal expansion so that the distributed thermal expansion term appearing in Eq. (1) is strongly suppressed in Eq. (2); we estimate its fractional contribution to be less than one part in 10^6, and so we ignore it in what follows.

The first term on right hand side in Eq. (2) indicates that the AOM frequency provides a high-quality readout of the resonator temperature if the thermooptic coefficient at f_1 and f_2 is sufficiently different to dominate over the noise terms, $\Gamma + N$. We show that this is the case for this resonator with sensing in the nK regime [31].

The experimental setup is shown in Fig. 1. A 5-mm-radius CaF_2 WG mode resonator is mounted on a piezoactuated translation stage within an acoustic and thermal shield. The laser light was coupled into the resonator using a high index prism. A conventional thermometer-heater pair was used to prestabilize the temperature of the system at the ± 0.1 K level. Light from a Nd:YAG laser at 1064 nm, together with its second harmonic at 532 nm (generated in a single-pass nonlinear crystal), was transferred into the shielded volume using single-mode optical fibers. The 532-nm light was double passed through an AOM to enable independent frequency tuning of this beam. The 1064-nm light was also double passed through a second AOM for reasons explained below. The two AOMs were driven with independent oscillators with nominal frequency around 80 MHz and were set to shift the frequency upward. Both beams were recombined inside the shielded volume using a dichroic filter before being coupled into the resonator. The transmitted beams were separated using a second dichroic filter and then registered by two photodetectors. The laser was frequency modulated at 1.638 MHz, and the two detected signals were synchronously demodulated using the traditional PDH technique to generate independent error signals appropriate to lock the laser signals onto their respective modes. The error signal generated from the 1064-nm mode was integrated and sent directly back to the laser controller to maintain the frequency lock. The second harmonic light was frequency locked by controlling the frequency of the synthesizer that drove the AOM.

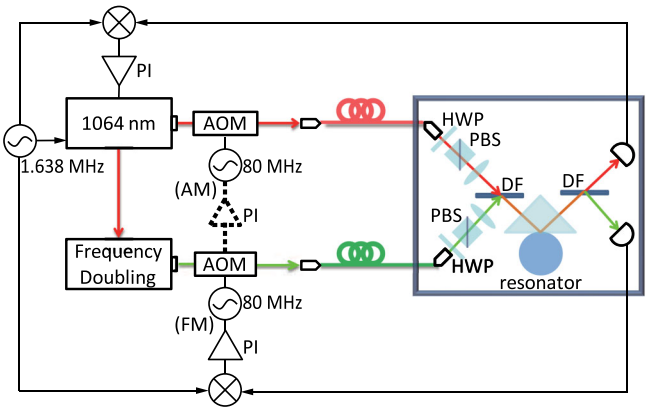

FIG. 1 (color online). Experimental setup. HWP: half-wave plate; PBS: polarizing beam splitter; DF: dichroic filter; AM: amplitude modulation; FM: frequency modulation; and PI: proportional-integral feedback. The dashed PI control part was only implemented when stabilizing the temperature of the resonator; i.e., it was not included in the temperature-sensing experiments.

As the evanescent field has different scale lengths for the two modes [29], it was necessary to overcouple the 1064-nm mode in order to achieve adequate coupling for the 532-nm mode. Thus, the loaded Q for the modes was 2.6×10^8 and 3.6×10^8 for the 1064- and 532-nm modes, respectively. This situation may be overcome by designing an appropriate coupling scheme [32].

The fast fluctuations of the WG-resonator thermometer were monitored by observing the frequency fluctuations of f_{AOM} with a spectrum analyzer, whereas slower fluctuations were monitored by a frequency counter. In addition, we measured the frequency of the lower frequency mode (f_1) with a stabilized frequency comb ($\Delta f/f < 10^{-13}$ for time scales > 1 s). For these experiments, the excitation power was deliberately kept at low levels (50 μW for 532 nm and 70 μW for 1064 nm) so that photothermal [16,33] and Kerr noise were both at least 10 dB below the measured f_{AOM} spectrum at all frequencies. The low levels of these noise sources during operation were verified by increasing the input power until both effects were observed and then turning the power back down by a factor of ten when in operation.

Figure 2 displays the variation of the lower mode frequency (f_1) as a function of the frequency of the AOM (a proxy for the mode temperature) where the resonator temperature drifts by 10 mK. As expected, there is a very high degree of correlation between f_1 and f_{AOM} (see inset), with slope $\Delta f_1/\Delta f_{\mathrm{AOM}} = 31.0$. The temperature sensitivity of the mode frequency can be calculated from the known parameter values for CaF_2 at 1064 nm ($n = 1.43$, $\beta = -11.4 \times 10^{-6}/\mathrm{K}$ and $\alpha = 18.7 \times 10^{-6}/\mathrm{K}$ at 1064 nm [34,35]) as $df_1/dT = -3.02$ GHz/K. We were able to verify this calculated value at the level of 10% by changing the temperature of the resonator mount intentionally. By combining the relationship seen in Fig. 2 with the calculated mode-temperature sensitivity we can get a thermometer calibration of $df_{\mathrm{AOM}}/dT = -97.42$ MHz/K. In what follows, we examine the fluctuations of f_{AOM} in more detail, but first we explain a means for temperature control of the resonator.

The resonator temperature can be controlled with a high bandwidth by actively controlling the input optical power.

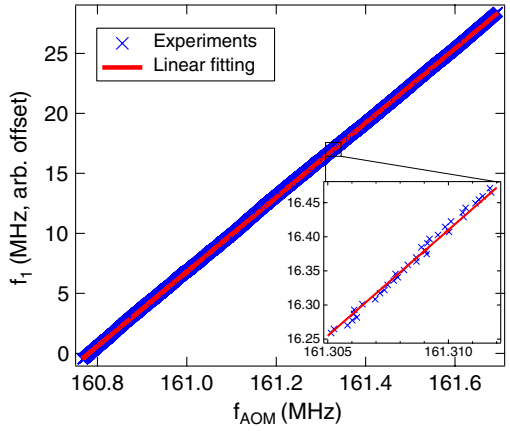

FIG. 2 (color online). Relation between f_1 and f_{AOM} while the resonator temperature drifts over 10 mK. The inset shows an enlarged fraction of the data. Decorrelation arises because the mode frequency depends on both the mode-averaged temperature as well as the entire temperature distribution, whereas the thermometer is only sensitive to the mode-averaged temperature.

For these experiments, we increased the 1064-nm power to ~2 mW to increase the range of the temperature control system. By directly measuring the transfer function between f_{AOM} and the 1064-nm power, we find the control bandwidth is > 1 kHz. The control actuator is indicated on Fig. 1 as the dotted line in which the drive power of the 1064-nm AOM is actively controlled to maintain the frequency of the AOM at a fixed value, which locks the resonator temperature. With this thermal control, the average mode temperature can be stabilized at the 100-nK level for more than an hour, as seen on Fig. 3(a). A residual

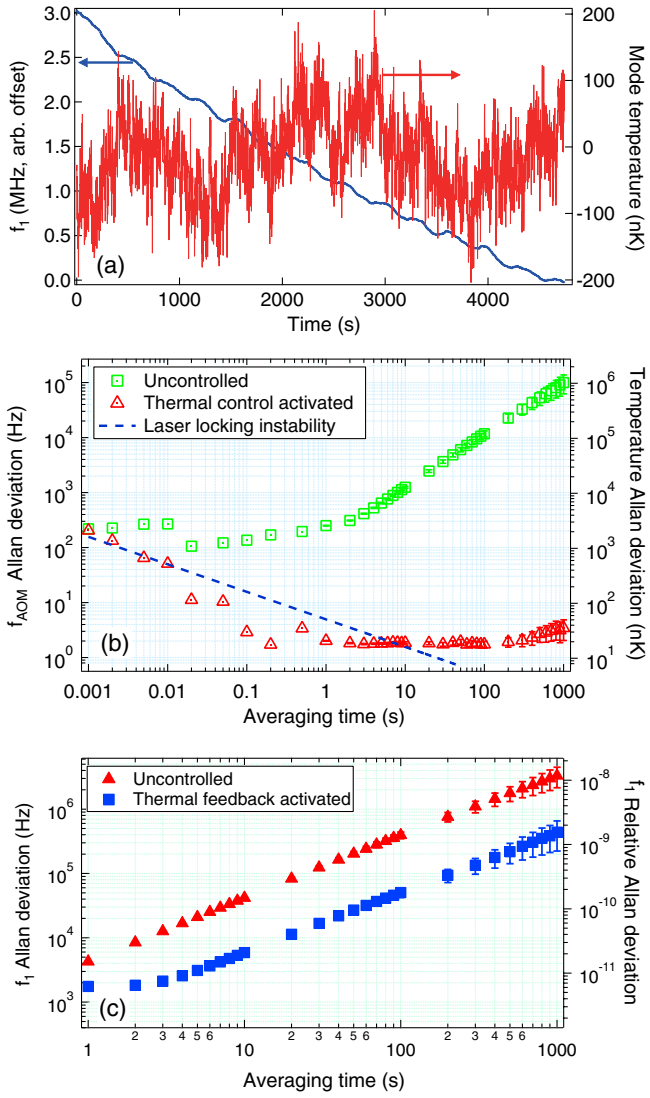

FIG. 3 (color online). (a) Mode frequency (f_1) and the mode temperature derived from f_{AOM} with thermal feedback control activated. (b) Allan deviations of f_{AOM} and the imputed mode temperature when temperature is uncontrolled (green squares) and actively controlled (red triangles). Dashed blue line is the estimated laser locking instability that limits the achievable mode volume temperature stability. (c) Allan deviation of the 1064-nm signal when the mode volume temperature is uncontrolled (red triangles) and actively controlled (blue squares).

drift of ~2.5 MHz/h in the mode frequency arises because this depends upon the entire temperature distribution, which is uncontrolled. The ripples with an ~300-s period are associated with room temperature modulation from the air-conditioning. Figure 3(b) shows a time-domain representation of the temperature fluctuations of the controlled and uncontrolled resonator using the Allan deviation [36]. We see that the control system suppresses the long-term temperature fluctuations by more than 4 orders of magnitude to the 30-nK level. The long-term temperature stability appears flat as a result of the interaction of the free running fluctuations and the transfer function of our control loop: a more sophisticated control system could result in further suppression. In Fig. 3(c), we show the Allan deviation of the locked 1064-nm mode frequency when the temperature is stabilized. The performance is substantially worse than one would expect if the mode frequency were only to depend upon the temperature in the mode ($\sim 5 \times 10^{-13}$ at 1-s averaging time). Nonetheless, the temperature control technique suppressed the mode frequency fluctuations by nearly 1 order of magnitude.

Figure 4 shows the power spectral density (PSD) of f_{AOM} when it is free running and when it is actively controlled. We also display the fundamental temperature fluctuations calculated using the method in [16]. We assume that the two optical modes have large spatial overlap, which is reasonable given that the thermal wavelength of even the highest frequency thermal noise (~1 kHz) considered here is much larger than the transverse extent of the optical modes, or their separation [16]. The unstabilized mode temperature fluctuation exceeds the calculated fundamental thermal fluctuations by a factor of 10 at low frequencies because the resonator is also subject to fluctuations in ambient temperature and input power.

Figure 4 also shows the noise floor of the temperature sensor [i.e., $N + \Gamma$ in Eq. (2)], which arises from the residual frequency noise in the two optical frequency

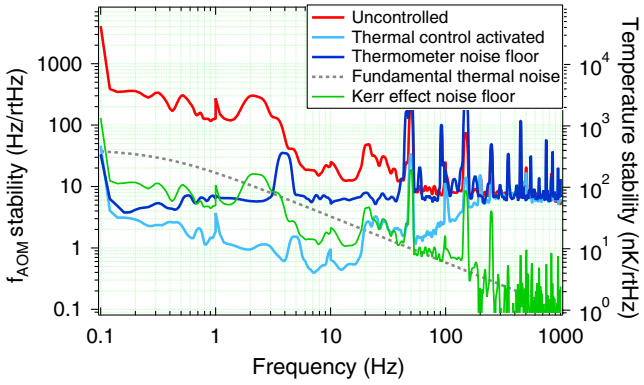

FIG. 4 (color online). PSD of f_{AOM} and its projected mode temperature. f_{AOM} is an in-loop signal that contains the lock instability noise, so below the lock instability noise floor (dark blue trace) the stabilized f_{AOM} PSD (light blue trace) does not project the real temperature PSD.

stabilization loops as well as the effect of Kerr fluctuations induced by the input intensity control. Residual frequency noise in the stabilization loops was independently estimated by measuring the noise in the frequency locking systems when the lasers were detuned from resonance: in these circumstances, we measure the sum of any electronic, shot noise, residual amplitude modulation, and residual intensity noise (RIN) that limit the frequency stabilization loops. The RIN in the environs of the PDH modulation frequency was seen to be the dominant contributor to this noise limit and sets a resulting 80-nK/$\sqrt{\mathrm{Hz}}$ temperature sensitivity that is reasonably frequency independent. It can be seen that this sensitivity is below the fundamental thermal noise of the resonator for thermal frequencies below 3 Hz.

Finally, Fig. 4 shows the residual temperature fluctuations once the mode temperature is stabilized: the fluctuations are strongly suppressed by the control system within its 200-Hz thermal control bandwidth.

We note that an additional noise floor arises when the resonator temperature is actively controlled: the required intensity modulation causes frequency shifts both through the desired temperature changes but also through an unwanted Kerr effect. This arises because the self-mode Kerr shift and cross-Kerr mode shift differ because of the differing cross-sectional areas for the two modes. This type of noise floor could be minimized by modulating the power of both excited modes together in a judiciously chosen ratio that results in the same effective Kerr shift in the two modes. We have not undertaken this procedure here since it was not the limiting factor in the performance of the temperature sensor. This induced noise floor is also shown on Fig. 4 and was determined by measuring the spectrum of the intensity modulation required to keep the temperature stabilized. The transfer coefficient between intensity and the resulting Kerr frequency shift was measured by applying an intentionally large intensity modulation. The resulting Kerr sensitivity was in broad agreement with the theoretical shifts expected from the relatively large mode volumes (~100 μm × 2 μm × 2 cm).

This experiment demonstrates the potential of the technique. There are several routes to further improve the sensitivity and resolution. (a) Reduce the residual noise in the frequency locking system by increasing the Q factor of the modes. To this end, a more sophisticated coupling would reduce the current difference in evanescent coupling strengths, thereby improving the Q factor [32]. (b) Increase the difference between the thermooptic coefficients for the fundamental and second harmonic by moving to fundamental wavelength of 800–900 nm. This difference can be approximately four times larger than that of the two wavelengths used here [37]. (c) Combine the wavelength- and polarization-dependent thermal-sensing techniques in a material such as MgF_2. Combining these approaches, we estimate that it is feasible to obtain a sensitivity below 10 nK/$\sqrt{\mathrm{Hz}}$ with the same detection noise.

To conclude, we report a dichroic mode temperature sensing and thermal stabilization scheme in a WG mode resonator. The experiment achieves tens of nano-Kelvin temperature stability by suppressing thermal fluctuations below the fundamental thermal noise level. This technique opens the possibility for the WG mode resonator as an ultrasensitive thermometer.

The authors gratefully acknowledge financial support from the Australian Research Council under Grants No. DP0877938, No. FT0991631, No. LE110100054, and No. LE100100009 that enabled this work. The authors also acknowledge the South Australian Government, who have provided generous financial support through the Premier's Science and Research Fund. The authors thank Ping Koy Lam for developing the facility for shaping the resonator and Frank Van Kann for useful discussions. W. W. gratefully acknowledges financial support from China Scholarship Council and University of Western Australia.

Note added in proof.—

We have recently implemented exactly the same scheme as described here on a MgF_2 resonator and achieved the predicted improvement in the sensitivity of the sensor to 30 $nK/\sqrt{Hz}$.

*wlweng@physics.uwa.edu.au

[1] L. D. Hansen and R. M. Hart, Thermochim. Acta **417**, 257 (2004).
[2] I. Wadsö, Thermochim. Acta **394**, 305 (2002).
[3] P. Richards, J. Appl. Phys. **76**, 1 (1994).
[4] H. Takesue, S. W. Nam, Q. Zhang, R. H. Hadfield, T. Honjo, K. Tamaki, and Y. Yamamoto, Nat. Photonics **1**, 343 (2007).
[5] M. Piat, J.-M. Lamarre, J. Meissonnier, J.-P. Torre, P. Camus, A. Benoit, J.-P. Crussaire, P. A. Ade, J. J. Bock, A. E. Lange *et al.*, in *Astronomical Telescopes and Instrumentation* (International Society for Optics and Photonics, Waikoloa, Hawaii, 2003), p. 740.
[6] S. I. Woods, S. M. Carr, T. M. Jung, A. C. Carter, and R. U. Datla, J. Appl. Phys. **108**, 024505 (2010).
[7] D. A. Sergatskov, P. K. Day, A. V. Babkin, R. C. Nelson, T. D. McCarson, S. T. P. Boyd, and R. V. Duncan, AIP Conf. Proc. **684**, 1009 (2003).
[8] A. G. Mann, C. Sheng, and A. N. Luiten, IEEE Trans. Instrum. Meas. **50**, 519 (2001).
[9] M. E. Tobar *et al.*, IEEE Trans. Ultrason. Ferroelectr. Freq. Control **53**, 2386 (2006).
[10] B. Sprenger, H. Schwefel, Z. Lu, S. Svitlov, and L. Wang, Opt. Lett. **35**, 2870 (2010).
[11] W. Liang, V. Ilchenko, A. Savchenkov, A. Matsko, D. Seidel, and L. Maleki, Opt. Lett. **35**, 2822 (2010).
[12] J. Alnis, A. Schliesser, C. Y. Wang, J. Hofer, T. J. Kippenberg, and T. W. Hänsch, Phys. Rev. A **84**, 011804 (2011).
[13] A. M. Armani, R. P. Kulkarni, S. E. Fraser, R. C. Flagan, and K. J. Vahala, Science **317**, 783 (2007).
[14] F. Vollmer, S. Arnold, and D. Keng, Proc. Natl. Acad. Sci. U.S.A. **105**, 20701 (2008).
[15] T. Kippenberg, R. Holzwarth, and S. Diddams, Science **332**, 555 (2011).
[16] A. B. Matsko, A. A. Savchenkov, N. Yu, and L. Maleki, J. Opt. Soc. Am. B **24**, 1324 (2007).
[17] T. Kessler, C. Hagemann, C. Grebing, T. Legero, U. Sterr, F. Riehle, M. Martin, L. Chen, and J. Ye, Nat. Photonics **6**, 687 (2012).
[18] S. Amairi, T. Legero, T. Kessler, U. Sterr, J. B. Wübbena, O. Mandel, and P. O. Schmidt, Appl. Phys. B **113**, 233 (2013).
[19] K. Numata, A. Kemery, and J. Camp, Phys. Rev. Lett. **93**, 250602 (2004).
[20] S. A. Webster, M. Oxborrow, S. Pugla, J. Millo, and P. Gill, Phys. Rev. A **77**, 033847 (2008).
[21] J. Millo, D. V. Magalhaes, C. Mandache, Y. Le Coq, E. M. L. English, P. G. Westergaard, J. Lodewyck, S. Bize, P. Lemonde, and G. Santarelli, Phys. Rev. A **79**, 053829 (2009).
[22] D. V. Strekalov, R. J. Thompson, L. M. Baumgartel, I. S. Grudinin, and N. Yu, Opt. Express **19**, 14495 (2011).
[23] I. Fescenko, J. Alnis, A. Schliesser, C. Wang, T. Kippenberg, and T. Hänsch, Opt. Express **20**, 19185 (2012).
[24] L. M. Baumgartel, R. J. Thompson, and N. Yu, Opt. Express **20**, 29798 (2012).
[25] A. A. Savchenkov, A. B. Matsko, V. S. Ilchenko, and L. Maleki, Opt. Express **15**, 6768 (2007).
[26] V. Braginsky, M. Gorodetsky, and S. Vyatchanin, Phys. Lett. A **264**, 1 (1999).
[27] M. L. Gorodetsky and I. S. Grudinin, J. Opt. Soc. Am. B **21**, 697 (2004).
[28] A. Schliesser, Ph. D. thesis, Ludwig Maximilian University of Munich, 2009.
[29] B. E. Little, J.-P. Laine, and H. A. Haus, J. Lightwave Technol. **17**, 704 (1999).
[30] R. Drever, J. L. Hall, F. Kowalski, J. Hough, G. Ford, A. Munley, and H. Ward, Appl. Phys. B **31**, 97 (1983).
[31] We note that suppressing mode-averaged temperature fluctuations using this technique does not significantly improve the absolute frequency stability of the WGM resonator. Equation (1) shows that the mode frequency depends on the temperature distribution throughout the resonator, which is not fixed by mode-averaged temperature control [23,24].
[32] M. Ghulinyan, F. Ramiro-Manzano, N. Prtljaga, R. Guider, I. Carusotto, A. Pitanti, G. Pucker, and L. Pavesi, Phys. Rev. Lett. **110**, 163901 (2013).
[33] K. Goda, K. McKenzie, E. E. Mikhailov, P. K. Lam, D. E. McClelland, and N. Mavalvala, Phys. Rev. A **72**, 043819 (2005).
[34] A. A. Savchenkov, A. B. Matsko, V. S. Ilchenko, N. Yu, and L. Maleki, J. Opt. Soc. Am. B **24**, 2988 (2007).
[35] A. Feldman, D. Horowitz, R. M. Waxler, and M. J. Dodge, *Optical Materials Characterization, Final Technical Report, February 1, 1978*, DTIC, 1979.
[36] D. W. Allan, Proc. IEEE **54**, 221 (1966).
[37] G. Ghosh, *Handbook of Optical Constants of Solids: Handbook of Thermo-Optic Coefficients of Optical Materials with Applications* (Academic Press, New York, 1998).